COMPUTATIONAL STUDIES ON HETEROGENIZATION OF HOMOGENEOUS CATALYST OF IRON(III), NICKEL(II) AND COPPER(II) N,N'-DISALICYLIDENE- 1,2-PHENYLENEDIAMINE COMPLEX

A THESIS

Submitted by

Manu Kumar

for the award of the degree

of

Master of Technology

(by research)

Department of Chemical Engineering

Indian Institute of Technology Madras

Thesis Certificate

This is to certify that the thesis titled **COMPUTATIONAL STUDIES ON HETEROGENIZATION OF HOMOGENEOUS CATALYST OF IRON(III), NICKEL(II) AND COPPER(II) N,N'-DISALICYLIDENE- 1,2-PHENYLENEDIAMINE COMPLEX**, submitted by **Manu Kumar**, to the Indian Institute of Technology, Madras, for the award of the degree of Master of Technology, is a bonafide record of the research work done by him under my supervision. The contents of this thesis, in full or in parts, have not been submitted to any other Institute or University for the award of any degree or diploma.

Prof Balasubramanian Viswanathan
Research Supervisor
Professor
Dept. of NCCR
IIT-Madras, 600 036
Place: Chennai

Acknowledgment

IIT Madras has been a wonderful place to be for the past two years. Here, I had the privilege of meeting some of the most beautiful persons who have contributed to making this a great experience and have enabled me to grow. Firstly, I would like to thank my thesis supervisor, **Prof Balasubramanian Viswanathan;** for his guidance throughout my research work and also for the encouragement and support he has provided me apart from academics. Through this project. I would also like to thank my friends: Naresh, Visnu, and Vikash for making my hostel life in IITM a memorable experience. I am also thankful to my lab mates: Nitika and Tamilmani ma'am for helping me out in my work and providing me with the good company throughout my graduate studies at IITM. Finally, I wish to acknowledge the support and great love of my parents and my siblings, who kept me going. This work would not have been possible without their emotional support.

Abstract

Density functional theory (DFT) calculations were carried out on iron(III), nickel(II) and copper(II) complexes of N,N'-ethylenebis (salicylimine) both at molecular level (isolated complexes) and encapsulated in a zeolite framework to investigate changes that occur in their geometrical and electronic parameters as well as in their reactivity and stability. The computational results showed that the zeolite encapsulated metal complexes have higher reactivity and less stability as compared to the isolated metal complexes.

KEY WORDS: Density functional theory, N,N'-ethylenebis (salicylimine), Computational studies, Heterogenization, Electronic parameters.

Table of Contents

List of Tables

List of Figures

INTRODUCTION

The catalyst is used for many industrial and related activities like food, chemical environment, medicine, etc. Owing to its different applications of catalyst synthesis or upgrading of the existed catalytic system is the hot research area. The present catalyst system is classified into homogeneous and heterogeneous based [1]. Transition metal-based complexes and organometallic compounds are examples of homogeneous catalysts. The transition metal-based homogeneous catalyst is a well-known catalytic system for different industrial applications. The effectiveness of the homogeneous catalyst is attributed to change in oxidation state of the central metal ion and the coordination environment of the ligand transition metal-based heterogeneous catalysts are normally solid species attached to an inorganic or organic solid surface [2]. Since the beginning of the twentieth century, both homogeneous and heterogeneous catalysts have been extensively used for the industrial applications. Though, the industrial applications of heterogeneous catalysis have grown at a faster rate than homogeneous catalysis. The problem associated with less interest in the homogeneous catalytic system is the difficulty of separation of catalysts from reaction medium and active site deactivation due the self-aggregation of the catalyst [3, 4, 5]. Therefore, applying of heterogenization process on the homogeneous catalytic system could bring the advantages of both homogeneous and heterogeneous systems. Several materials that can be employed for supporting homogeneous catalysts include zeolites, Nafion film or Nafion pallet, polyethylene copolymers, silica fabrics and clay etc. [6-7]. The unique characteristics of inorganic supporting materials linked to its flexibility and stability made them a good supporting or hosting medium Among the above inorganic hosting materials, zeolites are attractive micro porous supporting materials for the immobilization or encapsulation of transition metal complexes or organometallics within their cavities because it is cheap, naturally abundant and unique properties. The main problem in the preparation of zeolite encapsulated metal complexes is to identify suitable conditions at which well-defined distribution of transition metal complex happened in the zeolite cage, in its place of being concentrated on the zeolite external surface. Additionally, the encapsulation of metal complexes into zeolite cage helps to combine the characteristics of both neat zeolite and metal complex to obtain new hybrid catalysts [8]. Therefore, a comprehensive characterization of synthesized catalyst as compared to the neat metal complex and neat zeolite is necessary to ensure encapsulation process is properly established. The information we could able to extract from the existing physicochemical characterization techniques is limited. In general, zeolite encapsulated metal complexes are characterized to address the following aspects; the composition of metal complexes residing in the zeolite cage; the framework of zeolite is preserved after the encapsulation of metal complexes; thermal stability of the encapsulated metal complexes as compared to neat metal complexes and neat zeolite; morphological changes associated with encapsulation process; effect of molecular confinement on the conformational geometry and the mobility of the complexes inside the zeolite cage; internal versus external confinement and the distribution of guest compounds in zeolite host; nature of the metal complex formed in zeolite cavity compared to neat metal complex and neat zeolite; the effect of host-guest interactions on the structure of metal complex [8-10]. The existing physicochemical characterization techniques do not provide full information about the stability, reactivity, and proper inclusion of metal

complex inside the zeolite cage. Furthermore, it is not possible to have the information about the influence of the zeolite matrix on the structure and electronic properties of the enclosure compounds. However, a theoretical investigation of the physical and chemical properties-based quantum chemical calculations has provided a better understanding of the properties of neat metal complex and zeolite encapsulated metal complexes and the science behind their catalytic activity and stability [8-13]. Quantum chemical calculation based on density functional theory (DFT) is one of the operational tools in explaining chemical reactivity of the catalyst [14-18]. DFT calculation is also applied to understand the change in structural or geometrical parameters through calculations of bond length, bond angle and torsional angle of neat and encapsulated metal complexes [19, 20].Besides, the stability and reactivity of encapsulated complexes are investigated through highest occupied molecular orbitals (HOMO) and lowest unoccupied molecular orbitals (LUMO) energies of the metal complexes upon encapsulation into zeolite super cage [21, 22]. The encapsulation of the transition metal complexes inside the nano-pores of zeolite is one of the heterogenization methods [23-27]. Heterogenization is accomplished either by entrapping the metal complex within the zeolite nanocavities or by anchoring and/or tethering them to inert supportsc [28]. he structural design of zeolite-Y-based hybrid nano - catalysts via flexible ligand approach is convenient and ideal because the complex, once formed inside the cages of the zeolite is fitted suitable and not easily to diffuse out during the catalytic reaction [29, 30] The use of computational techniques in catalysis, homogeneous as well as heterogeneous, has become explored mainly because of the sophistication of several density functional theory software.

LITERATURE REVIEW

Computational details

On this study, the computational calculation was investigated using the density functional theory (DFT) approaches. For electronic and geometrical optimizations, generalized gradient approximation (GGA) and Perdew-Burke-Ernzerhof (PBE) exchange functional correlation were used along with double numerical (DN) basis set as implemented in the Dmol3 program The electronic density convergence threshold was set at 10^{-6} in the self-consistent field The optimization of geometrical parameters was executed with maintaining the value convergence thresholds for energy, force and atomic shifts about 10^{-5} Ha, 2×10^{-3} Ha/Å, and 10-3 Å, respectively. The electronic structure of homogeneous catalyst of Fe(III), Ni(II) and Cu(II)-Salophen complex as well as its heterogeneous catalyst associated with zeolite Y encapsulated respective metal complexes was calculated. Zeolite has well-defined three-dimensional rigid and stable structure having channels or cages which may be interconnected to form a multi-dimensional porous system of defined size [31-34], so that the encapsulation of Fe(III), Ni(II) and Cu(II)-Salophen complexes in these zeolite Y cavities allows the variation of their geometrical condition in a systematic method. The geometrical optimization of zeolite Y was investigated with fixing their super cage internal diameter and pore opening was about approximately 13.0 Å and 7.4 Å, respectively Since zeolite Y belongs to Faujasite family 48 tetrahedral units (48T) of the structure were used for a generation the given zeolite Y clusters with saturating them with hydrogen atoms.

Each of the terminal H atoms was optimized were fixed the framework of Si and O atoms of the clusters at their crystallographic positions. The encapsulated transition metal complexes inside the zeolite cage were optimized in repeatedly. During the optimization, terminated hydrogen atoms in the zeolite clusters are held fixed at their originally optimized positions.
electronic properties while heterogenization of the homogeneous catalyst of Fe(III), Ni(II), and Cu(II)-Salophen complexes using reactivity and stability parameters. The parameters of reactivity and stability such as global hardness (η) and chemical potential (μ) of the neat metal complex and zeolite Y encapsulated metal complex were calculated with applying DF Koopmans theorem using the presented Equation 1 and 2 [35];

$$\eta = \frac{E_{LUMO} - E_{HOMO}}{2} \quad (1)$$

$$\mu = \frac{E_{LUMO} + E_{HOMO}}{2} \quad (2)$$

where E LUMO is represents energy of the lowest unoccupied molecular orbital and E HOMO is also shows the energy of highest occupied molecular orbital. DFT based global descriptors such as global electrophilicity (ω) and global softness (s) was also calculated according to Parr *et al.* as shown in Equation 3 and 4 [36];

$$\omega = \frac{\mu^2}{2\eta} \quad (3)$$

$$S = \frac{1}{2\eta} \quad (4)$$

DFT

Density functional theory (DFT) describes the electronic states of atoms, molecules, and materials in terms of the three-dimensional electronic density of the system, which is a great simplification over wave function theory (WFT), which involves a 3N-dimensional anti symmetric wave function for a system with N electrons.1 Although DFT is sometimes considered the‘ ‘new kid on the block’’, it is now B45 years old in its modernformulation2 (more than half as old as quantum mechanics itself), and it has roots that are almost as ancient as the Schrodinger equation. DFT is almost always applied in the form introduced by Kohn and Sham,5 including its spin-polarized extension. The basic quantity in DFT is the many-electron spin density, r. The spin-polarized Kohn–Sham formalism involves a determinant formed from a set of N fictitious single-particle spin-orbitals corresponding to a non-interacting system of electrons with the same spin densities, r_a and r_b, as the real system, where r is the sum of r_a and

r_b, the spin density r_a is the 3-dimensional electron density of all spin-up electrons, and r_b is the same for spin-down electrons. In the original Kohn–Sham formalism (applicable to closed shell molecules and nonmagnetic solids), r_a equals r_b. (The original Kohn–Sham formalism may also be labeled spin restricted Kohn–Sham or restricted Kohn–Sham, and the spin-polarized version may be called spin-unrestricted or unrestricted.) We note that ‘‘spin density’’ is a generic term for the density associated with the subset of electrons characterized by the same definite value of S_z, i.e., either a or b say ‘‘spin-up density and spin-down density’’ rather than ‘‘spin densities’’). In a many-electron system comprised of both spin-up and spin-down electrons, the term spin-density is also sometimes used to refer to the position-dependent difference between the up and down spin densities, or to the vector analog of this quantity.

Density functional theory (DFT) has now become the preferred method for electronic structure theory for complex chemical systems, in part because its cost scales more favorably with system size than does the cost of correlated WFT, and yet it competes well in accuracy except for very small systems. This is true even in organic chemistry, but the advantages of DFT are still greater for metals, especially transition metals. The reason for this added advantage is static electron correlation.

INTRODUCTION TO FUNCTION

The oldest approximation is Dirac–Slater approximation to exchange [37, 38]. This must be renormalized for use with Kohn–Sham theory. This is now usually called the local the oldest approximation to a density functional is the spin density approximation (LSDA) since it depends only on spin densities (not their derivatives or orbitals). It can be derived from the exact exchange energy of a uniform electron gas (UEG), which is a somewhat unphysical system in which a constant electron density is neutralized by a constant background positive charge (rather than by discrete nuclear charges). The UEG correlation energy can be calculated numerically[39] and fit in various ways[40,41] and that leads to the LSDA for correlation, which has recently been thoroughly reviewed The next level of complexity in density functional is to add a dependence on the gradients of the spin densities; in particular the functional depends on the unit less reduced spin-density gradients, ss, which are proportional to |rrs|/r4/3 s .(Usually, though, we just say it depends on rrs.) Such functionals are called generalized gradient approximations (GGAs). Popular GGAs include BP86, where B denotes Becke’s 1988 exchange functional (usually abbreviated as B88 or just B),[42] and P86 denotes Perdew’s 1986 correlation functional;[44] BLYP, where LYP denotes the Lee–Yang–Parr correlation functional;[45]PW91, from Perdew and Wang in 1991;[46] and a functional of Perdew, Burke, and Ernzerhof (PBE)[47]. The modified Perdew–Wang functional of Adamo and Barone,[48] called mPWPW, is very similar to PBE. Notice that GGAs may combine an exchange functional from one source with a correlation functional from another, or they may both be from the same source. Thus BP86 and BLYP combine B88 exchange with P86 or LYP correlation, respectively; PW91 combines PW91 exchange with PW91 correlation; PBE combines PBE exchange with PBE correlation; mPWPW combines mPW exchange with PW91 correlation; SLYP combines the Slater LSDA exchange with LYP correlation; and PBELYP combines PBE exchange with LYP correlation. Density functional theory with LSDA or GGA functional includes self-exchange and self-correlation, both of which are unphysical. As a consequence, such functions tend to predict too small a HOMO–LUMO gap in molecules or too small a band gap in solids.

Furthermore, they tend to underestimate the relative stability of high-spin states in molecules or of high magnetic moments in solids. An important consequence of the error in LSDA and GGA exchange functional is that an electron interacts with its own charge density.
This unphysically raises the energy of localized states and causes DFT to produce excessively delocalized charge distributions [49-58] and to incorrectly predict some materials to be metals rather than insulators. Systems for which these errors are especially severe are sometimes called strongly correlated systems because delocalization is associated with the dominance of kinetic energy terms, and localization is associated with dominance by screened Coulomb potentials,[59] and electron correlation is important for electron localization because correlation

TYPES OF FUNCTION

1. local: LSDA approximation. Various approximations or fits to UEG exchange and correlation energies. (All LSDA functional are very similar, and in the present review we will not distinguish them.)
2. local: GGAs. BP86, SLYP, BLYP, PW91, PBE, PBELYP, mPWPW, mPWLYP.
3. nonlocal: hybrid GGAs. B3PW91, B3LYP, B1LYP, PBE0, MPW1K, B3LYP*, HSE.
4. local: meta GGAs. BB95, TPSS.
5. nonlocal: hybrid meta GGAs. B1B95, TPSSh.

RESULTS AND DISCUSSIONS

DFT studies on neat zeolite Y

Zeolite Y is made of SiO_4 and AlO_4 tetrahedra primary building blocks joined through oxygen bridges to form a three-dimensional structure having four or six-membered rings. The further interconnection of four- and six-membered rings also leads to the formation of the super cage. This super cage has a larger diameter among other cavities in the zeolite structure and it is the sole responsible for accepting the incoming transition metal complexes as a host. In accordance to this, the DFT calculation was used to create the optimized geometrical structure of the neat zeolite Y. Figure 1 shows the optimized DFT figure of neat zeolite Y and as shown in the figure the super cage is successfully formed having 13 Å and in the zeolite crystallographic T-site (T = Si or Al) and every Si atom links four types of the geometrical oxygen atom.

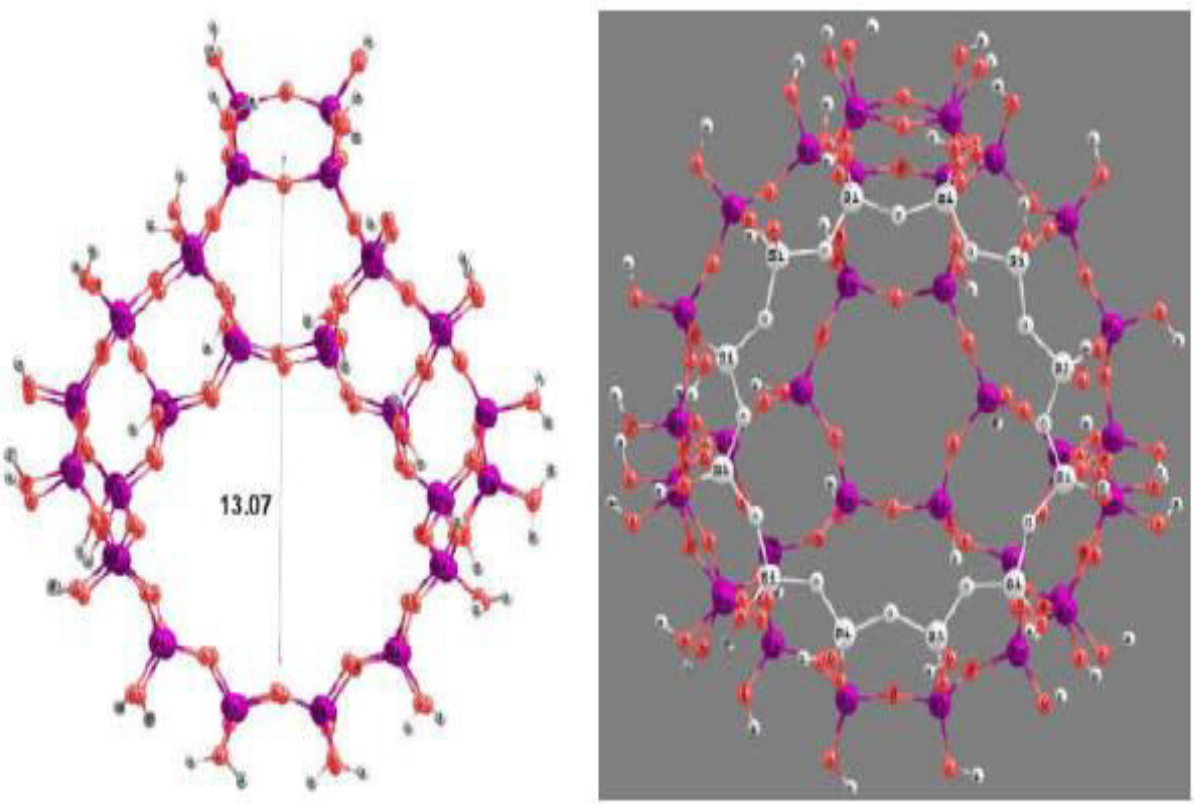

FIGURE 1 . The DFT optimized figure of neat zeolite Y

Geometrical optimization of metal complex and metal complex encapsulated into zeolite cage

The neat Salophen complex of Fe(III), Ni(II) and Cu(II) DFT geometrical parameters of bond length was compared with that zeolite Y encapsulated Fe(III), Ni(II) and Cu(II) Salophen complexes and it depicted in Table 1. The obtained optimized geometrical parameters of bond length difference of the neat and the encapsulated metal complex are relatively in good agreement. average bond length differences between homogeneous catalyst of Fe(III), Ni(II) and Cu(II) Salophen complexes and heterogeneous catalyst of Fe(III), Ni(II) and Cu(II) Salophen complexes after optimization were 0.070, 0.004 and 0.014 Å. bond length observed after encapsulation of for Fe(III), Ni(II) and Cu(II) Salophen complexes is attributed to the steric effect generated by the zeolite Y host material on the guest metal complexes.

Table 1 .The optimized bond length (in Å) for homogeneous and heterogeneous catalyst metal Salophen complexes, (M = Fe(III), Ni(II) and Cu(II)).

Bond type	**Fe(III)-Salophen complex**	**Fe(III)-Salophen complex in zeolite Y cage**	**Ni(II)-Salophen complex**	**Ni(II)-Salophen complex in zeolite Y cage**	**Cu(II)-Salophen complex**	**Cu(II)-Salophen complex in zeolite Y cage**
N_1-M	1.946	1.861	1.881	1.878	1.951	1.958
N_2-M	1.946	1.855	1.881	1.876	1.957	1.977
O_1-M	1.859	1.943	1.841	1.839	1.970	1.982
O_2-M	1.862	1.942	1.841	1.836	1.967	1.972
Cl-M	2.130	2.144			2.396	2.370

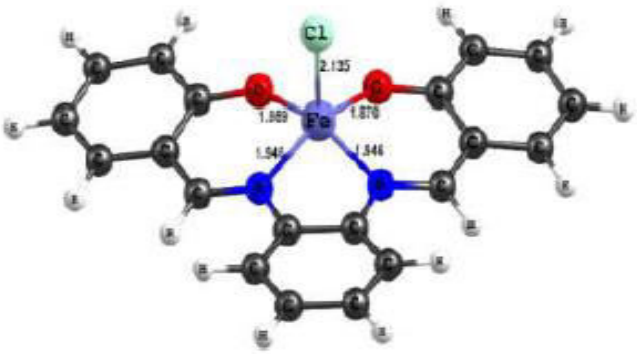

Fe(III)-Salophen complex

Fe(III)-Salophen complex in zeolite Y cage

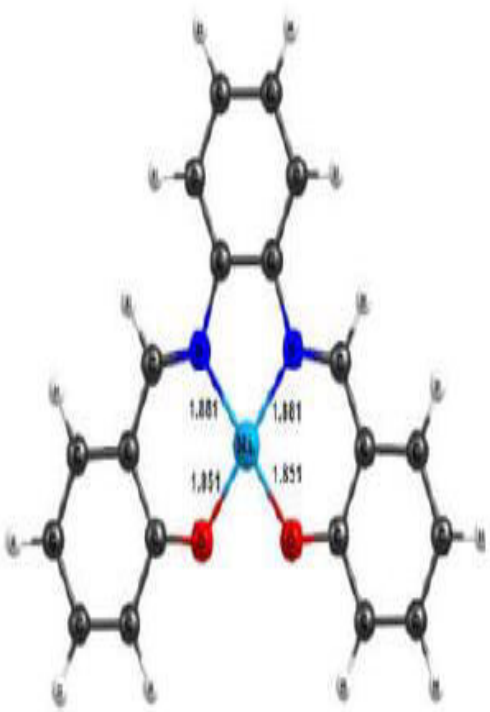

Ni(II)-Salophen complex

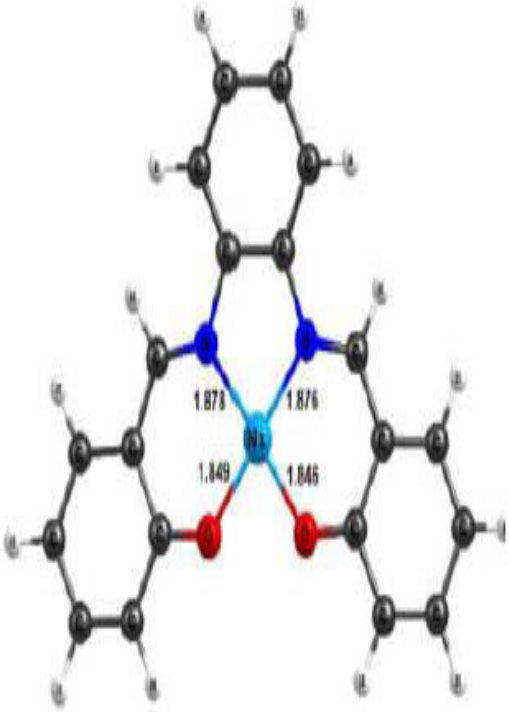

Ni(II)-Salophen complex in zeolite Y cage

FIGURE 2 shows the geometrical parameters obtained from Perdew-Burke-Ernzerhof (PBE) exchange functional correlation is used along with double numerical (DN) basis level calculations for the neat and encapsulated metal complexes.

Table 2. The optimized bond angles (in degree)

Bond type	Fe(III)-Salophen complex	Fe(III)-Salophen complex in zeolite Y cage	Ni(II)-Salophen complex	Ni(II)-Salophen complex in zeolite Y cage	Cu(II)-Salophen complex	Cu(II)-Salophen complex in zeolite Y cage
O_2-M-O_2	84.16	85.23	83.88	83.92	86.40	89.08
O_2-M-N_2	92.14	91.76	94.74	94.72	92.82	90.20
N_2-M-N_1	82.26	81.76	84.64		83.56	83.10
N_1-M-O_1	92.15	92.26	94.77		91.86	91.56
O_1-M-Cl	102	101.24			98.68	101.68
O_2-M-Cl	102.11	104.69			100.59	96.42
N_2-M-Cl	97.08	96.20			96.42	
N_1-M-Cl	97.10	95.43				

Torsional angle

C-O_1-M-Cl	-83.69	-80.74	-179.78	117.83	-67.36	-68.31
C-O_1-M-O_2	91.45	90.59	179.97	117.25	102.53	102.34
C-O_1-M-O_2	173.19	173.22	-0.03	-7.79	-169.50	-169.99
C-O_1-M-N_1	16.24	17.43	-179.94		28.20	31.14
C-O_2-M-Cl	83.77	84.23	179.98	9.67	75.06	65.14
C-O_2-M-N_2	-16.15			144.61	-22.16	-31.97
C-O_2-M-N_1	-91.42			-168.36		
C-O_2-M-O_1	-173.23					

TABLE 2 shows the optimized bond angle and torsional angle for Fe(III), Ni(II) and Cu(II) Salophen based complex of the homogeneous and heterogeneous catalyst. most of the optimized bond angles and torsional angle of neat metal complexes are slightly larger than the encapsulated one. complexes are existed in the different geometrical atmosphere.average optimized bond length changes observed between homogeneous and heterogeneous metal complexes catalyst after optimization is about 1.0, 0.1925 and 1.69 degree for Fe(III), Ni(II) and Cu(II) Salophen complexes. The bond angle, bond angle and torsional angle difference observed after encapsulation is associated with the existence of the metal complexes into different geometrical symmetry.

Optimization of metal complex and metal complex encapsulated into zeolite cage

The pattern and value of the highest occupied molecular orbital (HOMO) and the lowest Unoccupied molecular orbital (LUMO) for homogeneous and heterogeneous catalyst are shown in Figures 3, 4 and 5. the HOMO and LUMO energy of the zeolite encapsulated heterogeneous catalyst become destabilized and their energy increase in comparison to the homogeneous catalyst. The HOMOLUMO gap (ΔEH-L) of the heterogeneous catalyst of Fe(III), Ni(II) and Cu(II) Salophen complexes (Figures 3, 4 and 5) was found to decrease upon encapsulation. transfer of electrons from the heterogeneous catalyst of Fe(III), Ni(II) and Cu(II) Salophen complexes encapsulated into the zeolite cage is much more feasible than respective neat complexes.

Computational Studies on Heterogenization of Homogeneous Catalyst

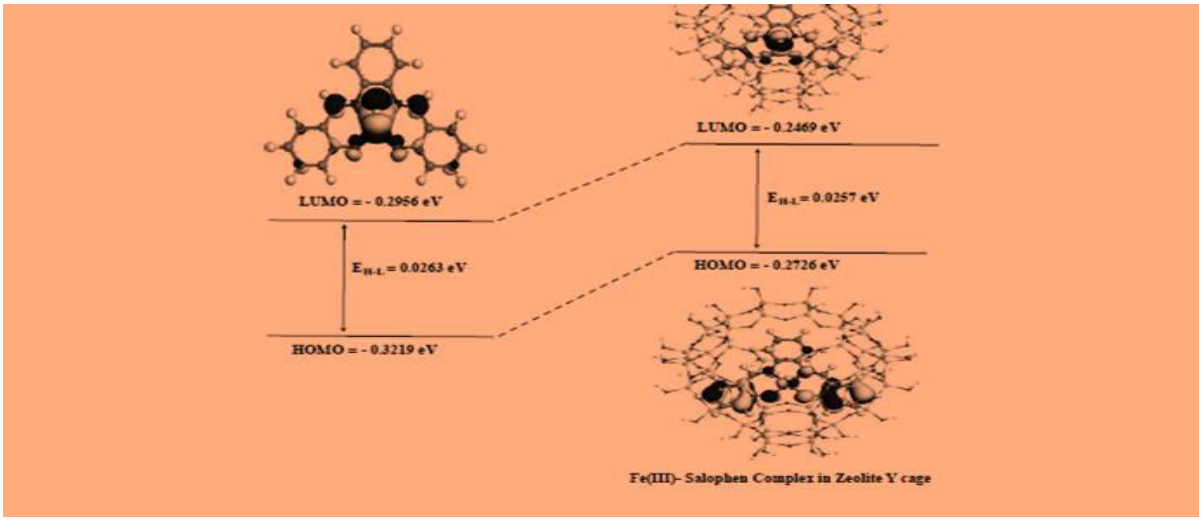

Figure 3 Schematic representation of HOMO-LUMO gap change for iron(III)-Salophen metal complex based homogeneous and heterogeneous catalyst

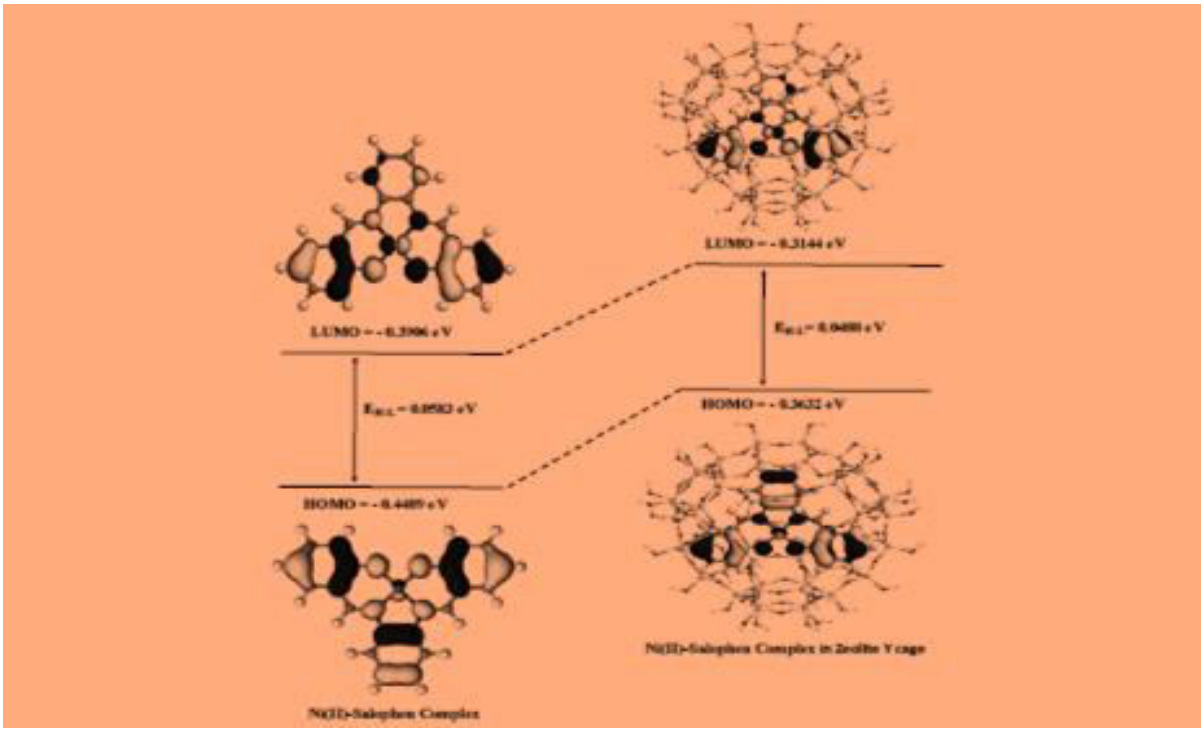

Figure 4 Schematic representation of HOMO-LUMO gap change for nickel(II)-Salophen metalncomplex based homogeneous and heterogeneous catalyst

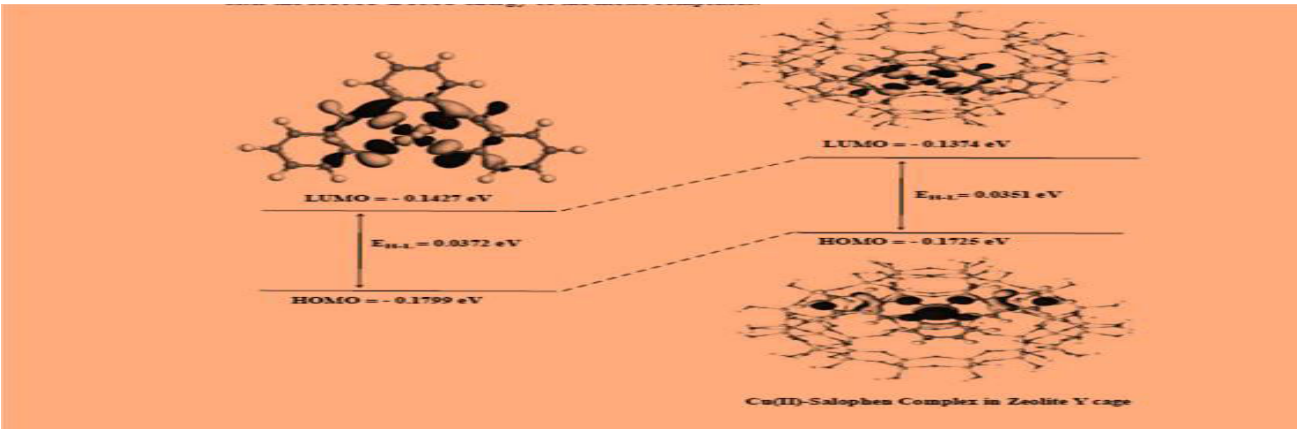

Figure 5 Schematic representation of HOMO-LUMO gap change for copper(II)-Salophen metal complex based homogeneous and heterogeneous catalyst.

Table 3 The calculated energy value of HOMO and LUMO (in eV), HOMO-LUMO gap (Δ*E*H-L, in eV),chemical potential (μ, in eV), global hardness (η, in eV) global electrophilicity (ω, in eV) and global softness (s, in eV) for homogeneous and heterogeneous catalyst

Sample	EHomo	ELumo	ΔEH-L	η	μ	ώ	s
Fe(III)-	-0.3216	-0.2953	.0260	0.0129	-0.3084	3.6243	38.0225

Salophen complex							
Fe(III)-Salophen complex in zeolite Y cage	-0.2723	-0.2463	0.0254	0.0125	-0.2594	2.6250	38.9102
Ni(II)-Salophen complex	-0.4486	-0.3903	0.0580	0.0289	-0.4194	3.0218	17.1524
Ni(II)-Salophen complex in zeolite Y cage	-0.3629	-0.3143	0.0485	0.0241	-0.3384	2.3519	20.4916
Cu(II)-Salophen complex	-0.1796	-0.1427	0.0369	0.0183	-0.1610	0.6991	26.8814
Cu(II)-Salophen complex in zeolite Y cage	-0.1725	-0.1373	0.0348	0.0173	-0.1546	0.6837	28.4917

CONCLUSIONS

The iron(III), nickel(II) and copper(II)-Salophen complexes based heterogeneous catalysts were successfully modeled and calculated in the zeolite super cage. DFT geometrical and electronic parameters such as bond distance, bond angle, torsional angle, HOMO-LUMO energy gap are changed once the metal complex is encapsulated into the zeolite pore. Furthermore, the calculated value of the DFT-global descriptors likel hardness, softness, electrophilicity and chemical potential computational results showed that the zeolite encapsulated metal complexes have higher reactivity and less stability as compared to the isolated metal complexes.

REFERENCES

1. Heveling, J. Heterogeneous catalytic chemistry by example of industrial applications. *J.Chem. Educ.* **2012**, 89, 1530-1536.
2. Kimura, E.; Sakonaka, A.; Machida R.; Kodama M.M. Novel nickel(II) complexes with doubly deprotonated dioxopentaamine macrocyclic ligands for uptake and activation of molecular oxygen. *J. Am. Chem. Soc.* **1982**, 104, 4255-4257.
3. Hailu, S.L.; Nair, B.U.; Redi-Abshiro, M.; Aravindhan, R.; Isabel, D.; Tessema, M. Oxidation of 4-chloro-3-methylphenol using zeolite Y-encapsulated iron(III)-, nickel(II)-, and copper(II)-N,N'-disalicylidene-1,2-phenylenediamine complexes. *Chin. J. Catal.* **2016**, 37, 135-145.
4. Robert, H.C. Deactivation in homogeneous transition metal catalysis: Causes, avoidance, and cure. *Chem. Rev.* **2015**, 115, 127-150.
5. Sherborne, G.J.; Chapman, M.R.; Blacker, A.J.; Bourne, R.A.; Chamberlain, T.W.; Crossley. B.D.; Lucas, S.J.; McGowan, P.C; Newton, M.A.; Screen, T.E.O.; Thompson, P. Activation and deactivation of a robust immobilized Cp* Ir-transfer hydrogenation catalyst: a multielement in situ x-ray absorption spectroscopy study. *J. Am. Chem. Soc.* **2015**, 137, 4151-4157.

6. Aravindhan, R.; Fathima, N.N.; Rao, J.R.; Nair, B.U. Wet oxidation of acid brown dye by hydrogen peroxide using heterogeneous catalyst Mn-salen-Y zeolite: a potential catalyst. *J. Hazard. Mater.* **2006**, 138, 152-159.
7. Kušić, H.; Koprivanac, N.; Selanec, I. Fe-exchanged zeolite as the effective heterogeneous Fenton-type catalyst for the organic pollutant minimization: UV irradiation assistance. *Chemosphere* **2006**, 65, 65-73.
8. Hailu, S.L.; Nair, B.U.; Redi-Abshiro, M.; Aravindhan. R.; Isabel, D.; Tessema, M.;Experimental and computational studies on zeolite-Y encapsulated iron(III) and nickel(II) complexes containing mixed-ligands of 2,2-bipyridine and 1,10-phenanthroline. *RSC Adv.* **2015**, 5, 88636-88645.
9. Jafarian, M.; Rashvand avei, M.; Khakali. M.; Gobal, F.; Rayati, S.; Mahjani, M.G. DFT and experimental study of the host–guest interactions effect on the structure, properties, and electro-catalytic activities of N2O2-Ni(II) Schiff-base complexes incorporated into zeolite. *Phys. Chem. C* **2012**, 116, 18518-18532.
10. Wannakao, S.; Khongpracha, P.; Limtrakul, J. Density functional theory study of thecarbonylene reaction of encapsulated formaldehyde in Cu(I), Ag(I), and Au(I) exchanged FAU zeolites. *J. Phys. Chem. A* **2011**, 115, 12486-12492.
11. Jafarian, M.; Rashvand avei, M.; Khakali. M.; Gobal, F.; Rayati, S.; Mahjani, M.G. DFT and experimental study of the host–guest interactions effect on the structure, properties, and electro-catalytic activities of N2O2-Ni(II) Schiff-base complexes incorporated into zeolite. *J. Phys. Chem. C* **2012**, 116, 18518-18532.
12. Hopmann, K.H.; Bayer, A. On the mechanism of iridium-catalyzed asymmetric hydrogenation of imines and alkenes: A theoretical study. *Organometallics* **2011**, 30, 2483-2497.
13. Václavík, J.; Kuzma, M.; Přech, J.; Kačer, P. Asymmetric transfer hydrogenation of imines and ketones using chiral RuIICl (η6-p-cymene)[(S, S)-N-TsDPEN] as a catalyst: A computational study. *Organometallics* **2011**, 30, 4822-4829.
14. Ganesan, R.; Viswanathan, B. Redox properties of bis(8-hydroxyquinoline) manganese(II) encapsulated in various zeolites. *J. Mol.Catal. A: Chem.* **2004**, 223, 21-29.
15. Bania, K.K.; Bharali, D.; Viswanathan, B.; Deka, R.C. Enhanced catalytic activity of zeolite encapsulated Fe(III)-Schiff-base complexes for oxidative coupling of 2-napthol. *Inorg. Chem.* **2012**, 51, 1657-1674.
16. Ozgur, A. FT-IR, Raman and DFT studies on the vibrational spectra of 2,2-bis(aminoethoxy) propane. *Bull. Chem. Soc. Ethiop.* **2016**, 30, 147-151.
17. Ye, Z.; Ting, L.; Qiwen, T. Theoretical study on electronic structures and spectroscopy of triarylborane substituted by thiophene. *Bull. Chem. Soc. Ethiop.* **2009**, 23, 77-83.
18. Özgür, A.; Cemal, P.; Mustafa, Ş. NMR spectroscopic study and DFT calculations of vibrational analyses, giao NMR shieldings and 1jch, 1jcc spin-spin coupling constants of 1,7-diaminoheptane. *Bull. Chem. Soc. Ethiop.* **2009**, 23, 85-96.
19. Han, L.H.; Zhang, C.R.; Zhe, J.W.; Jin, N.Z.; Shen, Y.L.; Wang, W.; Gong, J.J.; Chen, Y.H.; Liu, Z.J. Understanding the electronic structures and absorption properties of porphyrin sensitizers YD2 and YD2-o-C8 for dye-sensitized solar cells. *Int. J. Mol. Sci.* **2013**, 14, 20171-20188.

20. Mihaylov, T.; Trendafilova, N.; Kostova, I.; Georgieva, I.; Bauer, G. DFT modeling and spectroscopic study of metal-ligand bonding in La(III) complex of coumarin-3-carboxylic acid. *Chem. Phys.* **2006**, 327, 209-219
21. Ganesan, R.; Viswanathan, B. Physicochemical and catalytic properties of copper ethylenediamine complex encapsulated in various zeolites. *J. Phys. Chem. B* **2004**, 108, 7102-7114.
22. Ganesan, R.; Viswanathan, B. Redox properties of bis(8-hydroxyquinoline)manganese(II) encapsulated in various zeolites. *J. Mol. Catal. A: Chem.* **2004**, 223, 21-29.
23. L. H. Thomas, Math. Proc. Cambridge Philos. Soc., 1927, 23, 542.
24. E. Fermi, Z. Phys., 1928, 48, 73.
25. W. Kohn and L. J. Sham, Phys. Rev., 1965, 140, A1133.
26. U. von Barth and L. Hedin, J. Phys. C: Solid State Phys., 1972, 5, 1629.
27. A. K. Rajagopal and J. Callaway, Phys. Rev. B: Condens. Matter Mater. Phys., 1973.
28. D. R. Hartree, W. Hartree and B. Swirles, Philos. Trans. R. Soc. London, Ser. A, 1939, 238, 229
29. O. Sinanoglu and D. F. Tuan, J. Chem. Phys., 1963, 38, 1740.
30. D. G. Truhlar, J. Comput. Chem., 2007, 28, 73.
31. Liotta, L.F.; Gruttadauria, M.; Di Carlo, G.; Perrini, G.; Librando, V. Heterogeneous catalytic degradation of phenolic substrates: Catalysts activity. *J. Hazard. Mater.* **2009**, 162, 588-606.
32. Kesraoui-Ouki, S.; Cheeseman, C.R.; Perry, R. Natural zeolite utilisation in pollution control: A review of applications to metals' effluents. *J. Chem. Technol. Biotechnol.* **1994**, 59, 121-126.
33. Hernandez-Ramirez, O.; Holmes, S.M. Novel and modified materials for wastewater treatment applications. *J. Mater. Chem.* **2008**, 18, 2751-2761.
34. Hailu, S.L.; Nair, B.U.; Redi-Abshiro, M.; Aravindhan. R.; Isabel, D.; Tessema, M.; Experimental and computational studies on zeolite-Y encapsulated iron(III) and nickel(II) complexes containing mixed-ligands of 2,2-bipyridine and 1,10-phenanthroline. *RSC Adv.* **2015**, 5, 88636-88645.
35. Koopmans, T. Ordering of wave functions and eigenenergies to the individual electrons ofan atom. *Physica* **1933**, 1, 104-113.
36. Parr, R.G.; Chattaraj, P.K. Principle of maximum hardness. *J. Am. Chem. Soc.* **1991**, 113, 1854-1855.
37. P. A.M. Dirac, Math. Proc. Cambridge Philos. Soc., 1930, 26, 376.
38. J. C. Slater, Phys. Rev., 1951, 81, 385
39. D. M. Ceperley and B. J. Alder, Phys. Rev. Lett., 1980, 45, 566.
40. S. H. Vosko, L. Wilk and M. Nusair, Can. J. Phys., 1980, 58, 1200.
41. J. Perdew and Y. Wang, Phys. Rev. B: Condens. Matter Mater. Phys., 1992, 45, 13244.
42. A. D. Becke, Phys. Rev. A: At., Mol., Opt. Phys., 1988, 38, 3098.
43. J. P. Perdew, Phys. Rev. B: Condens. Matter Mater. Phys., 1986,33, 8822
44. C. Lee, W. Yang and R. G. Parr, Phys. Rev. B: Condens. MatterMater. Phys., 1988, 37, 785.
45. J. P. Perdew, in Electronic Structure of Solids ’91, ed. P. Ziesche and H. Eschrig, Akademie Verlag, Berlin, 1991, p. 11

46. J. P. Perdew, K. Burke and M. Enzerhof, Phys. Rev. Lett., 1996, 77, 3865.
47. C. Adamo and V. Barone, J. Chem. Phys., 1998, 108, 664.
48. M. H. Lim, S. E. Worthington, F. J. Dulles and C. J. Cramer,in Chemical Applications of Density Functional Theory,ed. B. B. Laird, R. B. Ross and T. Ziegler, American Chemical Society, Washington, DC, 1996, vol. 629, p. 402.
49. M. W. Nolan and G. W. Watson, J. Chem. Phys., 2006, 125,144701.
50. T. Bally and G. N. Sastry, J. Phys. Chem. A, 1997, 101, 7923.
51. C. J. Cramer and S. E. Barrows, J. Org. Chem., 1998, 63, 5523.
52. B. Braieda, P. C. Hiberty and A. Savin, J. Phys. Chem. A, 1998,102, 7872.
53. M. Sodupe, J. Bertran, L. Rodriguez-Santiago andE. J. Baerends, J. Phys. Chem. A, 1999, 103,166.
54. G. Pacchioni, F. Frigoli, D. Ricci and J. A. Weil, Phys. Rev. B:Condens. Matter Mater. Phys., 2000, 63, 054102
55. J. L. Gavartin, P. V. Sushko and A. L. Schluger, Phys. Rev. B:Condens. Matter Mater. Phys., 2003, 67, 035108.
56. J. Poater, M. Sola, A. Rimola, L. Rodriguez-Santiago and M. Sodupe, J. Phys. Chem. A, 2004, 108, 6072
57. M. Lundberg and P. E. M. Siegbahn, J. Chem. Phys., 2005, 122.
58. F. Lechermann, A. Georges, A. Poteryaev, S. Biermann,M. Posternak, A. Yamasaki and O. K. Andersen, Phys. Rev.B: Condens. Matter Mater. Phys., 2006, 74, 125120